**University Kasdi Merbah Ouargla**

**Faculty New Technologies Of Informatin And Communication**

**Department Of Electronics And Telecommunications**

# MEMORY OF ACADEMIC MASTER

**Domain:** Science and Technology

**Field:** Telecommunications

**Specialty:** Telecommunications Systems

**Prepared by:**

| | |
|---|---|
| **Hafiane Maroua** | **Ferkhi Kenza** |
| **Fellah Aicha** | **Bazzine Rania** |

**Theme:**

# Artificial Intelligence Based Tuberculosis Diagnosis

Publicly supported on: 25 June 2024

Before the jury:

| | | | |
|---|---|---|---|
| Dr. Lati Abdelhai | MCA | Supervisor | UKM OUARGLA |
| Dr. Bensid Khaled | MCA | President | UKM OUARGLA |
| Dr. Belkebir Djalila | MCA | Examiner | UKM OUARGLA |

Academic year: 2023/2024

# Abstract

Tuberculosis has seen a large spread in the world and is a serious and infectious disease. We have proposed a solution for the initial diagnosis of this disease. It is a Diatub application, based on artificial intelligence and its advanced techniques of deep learning and machine learning. The method of application is by imaging the lung X-ray and lifting it to the application, after which Diatub processes the image. The result is the patient's state of health if he is infected or healthy with a percentage as this does not take long, the result can be saved so as to inform the doctor and give the final diagnosis.



**Keywords:** tuberculosis, artificial intelligence, lung X-ray, deep learning, machine learning, Diatub.



# Résumé

La tuberculose s’est largement répandue dans le monde et constitue une maladie grave et infectieuse. Nous avons proposé une solution pour le diagnostic initial de cette maladie. C’est une application Diatub, basée sur l’intelligence artificielle et ses techniques avancées de deep learning et de machine learning. La méthode d’application consiste à imager la radiographie pulmonaire et à la soulever jusqu’à l’application, après quoi Diatub traite l’image. Le résultat est l’état de santé du patient s’il est infecté ou en bonne santé avec un pourcentage car cela ne prend pas longtemps, le résultat peut être enregistré afin d’informer le médecin et de donner le diagnostic final.



**Mots-clés:** tuberculose, intelligence artificielle, radiographie pulmonaire, apprentissage profond, apprentissage automatique, Diatub.



# ملخص

شهد مرض السل انتشار كبير في العالم و هو مرض خطير و معدي اقترحنا حل للتشخيص الاولي لهذا المرض و هو عبارة عن تطبيق Diatub, يعتمد على الذكاء الاصطناعي و تقنياته المطورة التي تتمثل في التعلم العميق و التعلم الالي. طريقة العمل بالتطبيق تكون بتصوير الاشعة السينية للرئة و رفعها للتطبيق و بعدها يقوم Diatub بمعالجة الصورة و النتيجة تكون عبارة عن الحالة الصحية للمريض اذا كان مصاب او سليم مع نسبة مئوية حيث لا يستغرق ذلك وقتا طويلا, يمكن حفظ النتيجة و ذلك لاطلاع الطبيب عليها و اعطاء التشخيص النهائي.



**الكلمات المفتاحية:** مرض السل, الذكاء الاصطناعي ,الاشعة السينية للرئة ,التعلم العميق, التعلم الالي,Diatub.

## Dedication

Thank God, who we look at today and thanks to him the long-awaited dream has become a reality after the fatigue and difficulties of five years of dream and science that carried the wishes of the night, today, we are on the threshold of graduation, picking the fruits of our tiredness and proudly lifting our hats

We direct this effort to those who have shown us the path of science, supported us and provided us with the means to succeed

To the light that illuminated our ways and embarrassed those whose names we bear with love and pride

**"Our parents"**

For those who facilitated adversity with their prayers and loving heart and enlightened our candles that .we had in dark nights the secret of our strength and success

**"Our mothers"**

For God's angels, we lived with them to learn through them the taste of beautiful life, those angels who changed the concept of love, friendship and bonds in our lives

**" Our sisters and brothers"**

For those who overwhelmed us with love and advice gave us strength and were the target of knowing the meaning of friendship through them

**"Our friends"**

The journey wasn't short, the dream wasn't close, the road wasn't crowded with facilities, but we did.

## Acknowledgment

first of all we would like to thank Allah the Almighty for giving us the courage and willingness to complete this work

We particularly want to thank our supervisor **Dr.Lati abdelhai** professor at U.K.M Ouargla for your supervision, advices, comments and kindness. We would also like to thank **Mr.Bekkari Lakhdar** for helping us throughout the realization of this thesis

we also thank the members of the jury president **Dr.Bensid Khaled** and examiner **Dr.Belkebir Djalila** who kindly read and examine our work

a special thank you to all those who supported us to complete this work

# List of abbreviations

AI:  Artificial Intelligence.

APP: Application

CNN: Convolutional Neural Networks.

CPU: Central Processing Unit.

CXR: Chest X-ray.

DL: Deep Learning.

DNN: Deep Neural Networks.

FC: Fully Connected.

FN: False Negative.

FP: False Positive.

GPU: Graphics Processing Unit.

IGRA: Interferon Gamma Release Assay.

MAP: Mean Average Precision.

ML: Machine Learning.

RGB: Red Green Blue.

TB: Tuberculosis.

TL: Transfer Learning.

TN: True Negative.

TP: True Positive.

VGG: Visual Geometry Group.

YOLO: You Only Look Once.

# List of Contents

# List of figures

# List of Tables

# General Introduction

# General Introduction

In our time, the world has known a great development in the field of technology, automation and the development of advanced computing and data transfer is a branch of knowledge based on innovation and the use of modern technical means. The role of technology is linked to our daily lives, society and the surrounding environment. Technology can be defined as a way to accomplish a task using multiple means, technical methods and knowledge and has too much on the educational process. Since the introduction of the Internet, colleges and graduate programs have been offering online learning platforms.

It aims to develop systems capable of simulating human mental abilities, such as learning, thinking, and decision-making. AI is increasingly used in technology development. For example, artificial intelligence can improve systems performance, analyze large data and improved safety and has an impact in several areas including health. AI has become a critical tool for medical professionals, Machine learning and deep learning techniques are widely used in radiography and pathology such as infectious diseases that pose a global threat disease ", where the disease can spread rapidly, including tuberculosis, where it also enhances the accuracy of the diagnosis. AI can reduce human errors, support medical professionals, and provide 24/7 patient services.

Our project's goal is to automatically detect tuberculosis by analyzing images using lung radiography (CXR). One potential use of this research is to speed up the diagnosis of the disease based on radiation image analysis without the need for expensive medical tests.

In the first chapter we touched on the concept of tuberculosis, which is an infectious and serious disease caused by Mycobacteria tuberculosis that affects any part of the body such as the lung, kidneys, brain and lymphoma and we also touched on its symptoms, its types and how it is diagnosed classically and newly.

In second chapter, we touched on the concept of artificial intelligence and its branches, its uses in the field of health, learning transmission networks and mechanisms (VGG-16, VGG-19, ResNet50 and YOLOv8).

In chapter III, we discussed the results of tuberculosis data training on previous networks and the analysis of the resulting curves, finally, we talked about our project of applying the initial diagnosis of tuberculosis by raising X-rays or taking them on camera. Here lies the role of deep learning in the processing of data. Its outputs are the same radioactive section defined in a box in addition to that classification whether normal or tuberculosis with a ratio.

# Chapter I

## Tuberculosis Disease and its Diagnosis

# I.1. Introduction

TB is an infectious disease caused by a bacterium known as "TB microbacterium." It can be diagnosed through phlegm screening, lungs X-rays, skin tests, or blood test to detect the presence of bacteria and there are modern diagnostic methods such as image processing using artificial intelligence. In this chapter we will talk about the concept of tuberculosis in detail as well as its symptoms and types.

## I.2. Brief History

As centuries and millennia passed, human beings began to live in larger and larger communities, and with this shift came environmental changes that were associated with a change in the delicate balance between humans and the tubercle bacillus. Two alternative theories have been proposed to explain the epidemic spread and subsequent decline of tuberculosis that followed. In the 1700s and early 1800s, tuberculosis prevalence peaked in Western Europe and the United States and was undoubtedly the largest cause of death, and 100 to 200 years later, it had spread in full force to Eastern Europe, Asia, Africa, and South America. The epidemic grew over the next two centuries and spread through Western Europe. During this phase of the epidemic, almost all Western Europeans became infected with M. tuberculosis, and about one in four deaths were due to tuberculosis. Army medical officers from Great Britain noted that tuberculosis was unknown in those parts of Africa where European immigration had not occurred. By matching microbial drug susceptibility patterns, one patient with tuberculosis laryngitis was identified as particularly infectious. Modern parallels are presented by micro-epidemics in poorly ventilated areas, of which few are more dramatic than the one described by Catanzaro just 100 years after Koch's demonstration of the tubercle bacillus. [1]

## I.3. Definition of tuberculosis

Mycobacterium tuberculosis complex organisms are the source of tuberculosis (TB), an infectious disease spread by the air. Despite being a pulmonary infection first and foremost, Mycobacterium TB can infect nearly every area of the body. A latent tuberculosis infection, in which the bacteria are contained within granulomas, can progress from containment in the host to an infectious stage, where the patient exhibits symptoms such as fever, chills, coughing, and weight loss. Contagion only exists with active pulmonary TB. TB is still a leading cause of morbidity and death in many low- and middle-income nations, and drug-resistant TB is a significant problem in many contexts. While a number of novel TB diagnostics, such as fast molecular tests, have been created, there is still a need for. [2]

**Figure I.1: X-ray image of tuberculosis-sick lung. [3]**

## I.4. Types of pulmonary tuberculosis

The patient's age and the infection's stage both affect where the infection is located in the lung: In infants, the original infection can occur anywhere in the lung, whereas in adults, the upper or lower zone is more likely to be affected.

In contrast, post-primary infections strongly favor the upper zones.

The spread of miliary TB is uniform in both lung

### I.4.1. Primary TB in the lungs

The initial site of infection in primary pulmonary tuberculosis can be anywhere in the lung and present in a variety of non-specific ways, such as being too tiny to be seen or having patchy patches of consolidation or even lobar consolidation. Of adults, 90% have radiographic signs of parenchymal infection, and 70% of children do as well. Cavitation occurs in only 10–30% of cases of primary TB. Most of the time, the infection becomes localized and develops into a tuberculoma, or caseating granuloma. This tumor typically calcifies and becomes known as a Ghon lesion.

### I.4.2. Post-primary TB of the lungs

Post-primary TB, sometimes referred to as secondary tuberculosis or post-primary pulmonary tuberculosis, develops years later and is often associated with weakened immunity. Most often, post-primary TB in the lungs occurs in any of the following ways:

-The higher lobes' posterior portions

-The upper portions of the lower lobes

Post-primary tuberculosis is characterized by poorly defined linear and nodular opacities or patchy consolidation.

In 20–45% of instances, post-primary infections are found, and they have a considerably higher chance of becoming cavitative than primary infections. They form in the posterior portions of the upper lobes in the great majority of instances (85%) 1, 7. There is a chance of contagion since the establishment of an air-fluid level suggests communication with the airway. A quite typical observation is endobronchial spread in adjacent airways, which results in branching lesions or relatively well-defined 2-4 mm nodules (also known as the "tree-in-bud sign").

Hurdle nodal enlargement is observed in about one-third of patients. Although they are less frequent, lobar consolidation, tuberculoma development, and miliary TB are other acknowledged patterns of post-primary TB. Only 5% of post-primary TB cases are tuberculomas, which manifest as a well-defined, spherical mass that is usually found in the upper lobes. Eighty percent of them are solitary, and they can grow up to 4 cm in size.

### I.4.3. Miliary tuberculosis in the lungs

Although rare it, milder forms of tuberculosis have a dismal prognosis. It symbolizes the hematogenous spread of an unchecked tuberculosis infection. Both primary and post-primary TB cases exhibit it. The lungs are typically the easiest organ to visualize, despite the fact that implants are found throughout the body.

Miliary deposits show up as consistently sized, uniformly scattered nodules with a diameter of 1-3 mm. If the therapy is effective, the residual anomaly disappears. [4]

## I.5. Symptoms of tuberculosis

The majority of the time, symptoms are modest and appear gradually over weeks, months, or even years. Initially, symptoms of tuberculosis are frequently misdiagnosed as allergies, smoker's cough, or persistent bronchitis brought on by a cold or virus. Although it can cause issues in other sections of the body, tuberculosis infections often affect the lungs. The following are typical signs of tuberculosis in the lungs:

- A cough that lasts longer than three weeks
- An inexplicable loss of weight
- Fever of low grade
- Sweating at night

See your healthcare practitioner if you experience any of these symptoms. [5]


**Figure I.2: Tuberculosis symptoms. [6]**

## I.6. Diagnosis of tuberculosis

Testing for TB risk individuals Positive screening test results might occasionally be the first sign of tuberculosis. Individuals who are at risk of tuberculosis get routine screening tests for the disease. Physicians may have a suspicion of tuberculosis if they observe symptoms including fever, coughing up blood, night sweats, weight loss, chest pain, and dyspnea that lasts longer than two to three weeks. These tests include:

- Blood testing or skin tests for tuberculosis
- Chest x-ray diagnosis [7]

### I.6.1. Classical diagnosis methods

#### I.6.1.1.Interferon Gamma Release Assay (IGRA)

An individual with a TB bacterial infection can be identified by a blood test called an IGRA. To find out how successfully a subject's immune system fights against TB bacteria, an IGRA checks the subject's blood in a lab. [8]

**Figure I.3: Blood testing for tuberculosis. [9]**

### I.6.1.2 Skin testing for tuberculin

To determine whether someone has been exposed to the TB germs, one can do the mantoux tuberculin skin test. The immunological response of a patient to M. tuberculosis antigens (tuberculin) is measured by this test. Two or three days after a tiny dose of tuberculin is injected intradermally, the skin response is assessed. If a positive reaction is defined as 5 mm of induration, the test can identify tuberculosis in healthy individuals with high sensitivity. Nevertheless, a number of illnesses, such as active tuberculosis, cause erroneous negative results. [10]

**Figure I.4: Skin testing for tuberculin.[11, 12]**

### I.6.1.3. Chest x-ray diagnosis

A fast imaging technique called a chest X-ray (CXR) can identify abnormalities in the lungs. A CT scan can be used to diagnose conditions related to the thoracic cavity, which includes the heart, diaphragm, lungs, ribs, and airways.CXR has historically been one of the primary techniques for diagnosing tuberculosis (TB), especially pulmonary TB. Computed tomography (CXR) is a useful diagnostic technique for patients to rule out tuberculosis (TB) because of its high sensitivity for pulmonary TB. This is especially true when the X-ray is analyzed to check for any anomalies that would be compatible with TB.

However, CXR has low specificity; many other lung pathologies also show CXR abnormalities that are consistent with pulmonary tuberculosis and, therefore, may be indicative of other pathologies in addition to TB. Certain scan abnormalities, such as cavities, are highly specific to pulmonary tuberculosis.

Moreover, there are significant variations in how observers perceive CXRs from one observer to another. Relying only on CXR for tuberculosis diagnosis leads to both overdiagnosis and underdiagnosis. [13]

### I.6.2. Modern diagnosis methods

Although there are classic methods for identifying tuberculosis, there are modern methods that help identify it in a short time, including image processing.

### I.6.2.1. image processing

Image processing is the process of taking an image, converting it to digital format, and then applying various adjustments to it to produce an improved image or extract some valuable information. It's a kind of signal distribution where a picture serves as the input and an image or attributes related to that image serve as the output. [14]

**Image filtering:**

Image filtering is a basic procedure that enhances the perception of certain features, reduces noise, and compensates for certain sensor faults by eliminating disruptive or inconsequential elements from digital images.

Reducing the disparities in intensity within each image is the goal of filtration. The image must be governed while maintaining the viewer's integrity, with transfers between homogeneous areas and significant features needing to be preserved to the greatest extent possible.

**Note:** Every contender aims to lessen a particular kind of flaw. No universal candidate can fully fix every flaw. Select the appropriate filters according to the flaws that need to be fixed.

A variety of filters are employed in image processing, and they fall into two groups:

**linear filters stationary**

- Medium filter.
- Gaussian filter.

**Nonlinear filters stationary**

- Median filter. [15]

## I.7. Uses of artificial intelligence in the field of medicine

Medical Care. Health facilities can use a wide range of AI apps to do many routine duties. AI systems, for instance, are able to ―read‖ patient X-ray readings and tailored medication data for a variety of illnesses (such as low-dose computed tomography scans for lung cancer, data from radiomics and biopsy slides, and breast mammograms). AI is also capable of serving as a personal healthcare assistant. For instance. AI can serve as a life coach, reminding patients to take their medications, reminding people to exercise and how long to do so, or suggesting nutritious diet to prevent obesity. [16]

## I.8. Conclusion

In this chapter we touched on the concept of tuberculosis and how to detect it in both classic and modern ways and the uses of artificial intelligence in the field of medicine, in the next chapter we will learn about artificial intelligence and its branches.

# Chapter II

## Transfer learning Based Tuberculosis Diagnosis

# II.1. Introduction

Artificial Intelligence (AI) is a transformative technology that rapidly shapes our world. It enables machines to perform human-like tasks, from identifying speech and images to making complex decisions. Artificial intelligence has the potential to revolutionize industries, solve global challenges, and enhance our daily lives. In this chapter, we will study the concept of artificial intelligence and its branches and transfer learning networks as VGG16, VGG19, ResNet50 and YOLOv8.

## II.2. A brief introduction to AI

Emeritus Stanford Professor John McCarthy first used the term **artificial intelligence (AI)** in 1955, and he defined it as "the science and engineering of making intelligent machines." Currently, we emphasize robots that can learn, at least partially like people do. A lot of research has included humans programming machines to act in smart ways, such playing chess. [17]

**Machine Learning (ML)** Automatic learning refers to the use of artificial intelligence that gives systems the ability to learn and improve on their own through experience without explicit programming. It appears focuses mostly on creating sophisticated programs and models that are challenging to implement using conventional methods. It also makes it easier to analyze enormous amounts of data. Additionally, this method yields much faster and more effective results for identifying profitable opportunities or dangerous risks related to specific problems. Combining AI, cognitive technologies, and automatic learning can further increase its effectiveness in handling large amounts of data. [18]

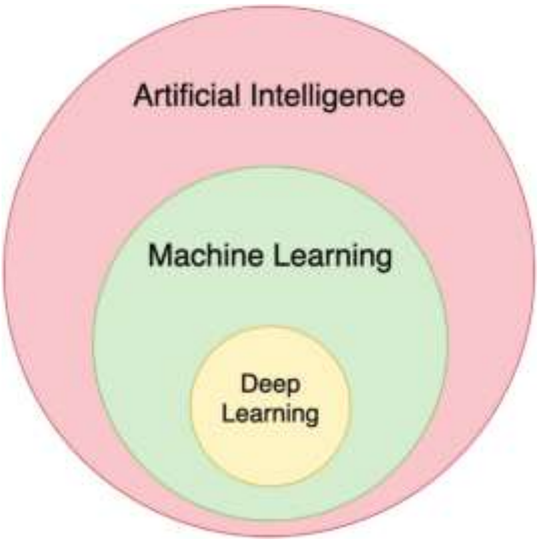


**Figure II.1: Artificial intelligence and subdisciplines. [19]**

**Deep learning (DL)** It is the branch of artificial intelligence that mimics how the human mind processes information, makes decisions based on examples, and applies that knowledge. Why deep learning, and how does it get applied? The amount of raw data available on various websites, such as online media and corporate websites, is rapidly increasing worldwide. This data is sometimes referred to as big data.This is unstructured and can take a very long time for someone to extract the relevant information from. Here, the concept of profound learning is applied in order to extract the important knowledge**.** [20]

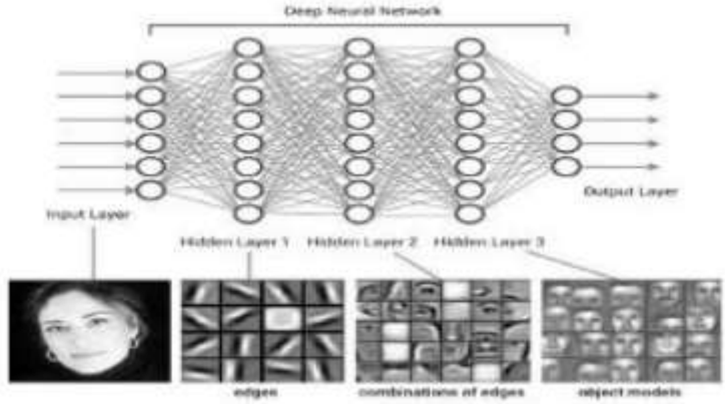


**Figure II.2: Layers of Deep Learning.**

## II.3. CNN Convolutional Neural Network

Inspired by the structure of animal visual cortex, CNN is a form of deep learning model for processing grid-patterned data, such photographs. It is made to automatically and adaptively learn spatial hierarchies of characteristics, from low- to high-level patterns. Convolution, pooling, and fully connected layers are the three main types of layers (or building pieces) that make up a CNN in mathematics. While the third layer, a fully linked layer, translates the extracted features into the final output, like classification, the first two layers—convolution and pooling—perform feature extraction. A crucial component of CNN is the convolution layer. CNN is made up of a series of mathematical operations, including convolution, a particular kind of linear operation. A small grid of parameters called a kernel, an optimizable feature extractor, is applied at each image position in digital images. This makes CNNs highly efficient for image processing because a feature may occur anywhere in the image. Pixel values are stored in a two-dimensional (2D) grid, or an array of numbers (Fig II.3). Complexity in retrieved characteristics can grow hierarchically and progressively as one layer feeds its output into the next layer. Training is the process of fine-tuning parameters, such kernels, using optimization algorithms like gradient descent and backpropagation, among others, to minimize the difference between outputs and ground truth labels. [21]

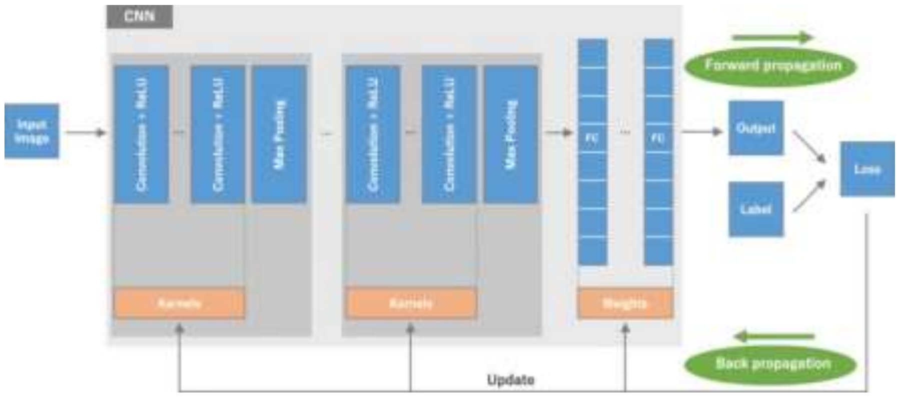


**Figure II.3:** **Convolutional neural network (CNN) architecture and the training process.**

### II.3.1. Convolution Layers

The central element of any CNN architecture is the convolutional layer. It has a collection of convolutional kernels, sometimes referred to as filters, which convolve the input image using N-dimensional metrics to produce an output feature map.

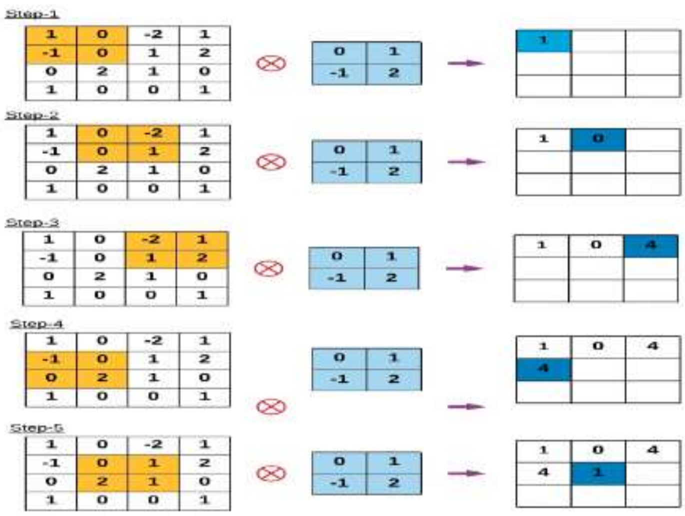


**Figure II.4: 5 steps of convolution operation.**

### II.3.2. Pooling Layers

The feature maps (created following convolution operations) are sub-sampled using the pooling layers; that is, the bigger feature maps are shrunk to smaller feature maps. In every pool phase, the most prominent features (or information) are preserved while the feature maps are shrunk. As with the convolution operation, the pooling operation is carried out by defining the operation's stride and pooled region size. Different pooling approaches, such as max pooling, min pooling, average pooling, gated pooling, tree pooling, etc., are employed in different pooling layers. The most often used and well-liked pooling technique is max pooling. The primary disadvantage of the pooling layer is that it might occasionally cause CNN's overall performance to decline .This is because, without regard to the feature's precise location, the pooling layer aids CNN in determining whether a certain feature is present in the input image. [22]

#### II.3.2.1. Average Pooling Layer

The first convolution-based deep neural network was created using the average for feature extraction and pooling. An average pooling layer divides the input into rectangular pooling regions and calculates the average values of each zone, as seen in Fig. 1, to perform down-sampling.

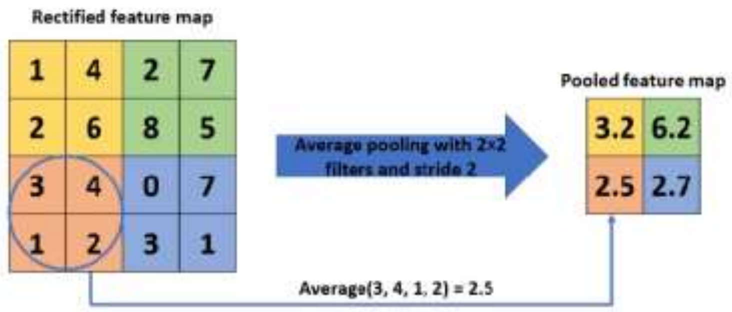


**Figure II.5: Example of Average Pooling operation.**

#### II.3.2.2. Max Pooling Layer

The convolutional output bands can be down-sampled using a max-pooling technique, which lowers variability. In a set of $R$ activations, the max-pooling operator forwards the maximum value. The $\boldsymbol{T}$-th max-pooled band is made up of filters connected to $J$. [23]

$pm$ = [$p$],,.. $pj$, $m$,.., $pJ$,$m$] ∈ $R$j

$$pj, = \max(hj, (m-1) + r)$$

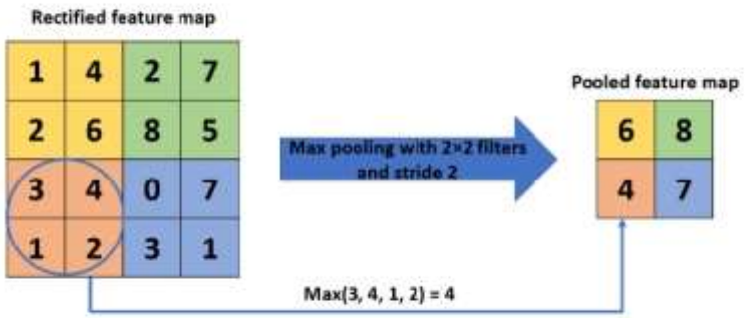


**Figure II.6: Example of Max-Pooling operation.**

## II.4. Deep neural networks

DNNs are extensively utilized in data-driven modeling. A DNN is made up of layers with mathematical interactions between nodes and edges. Backpropagation is used to update these associations during data training. The updated relationships serve as the formulas for forecasting the output variables depending on the input variables after training. Consequently, a key benefit of DNNs is their ability to represent the relationships present in a system, irrespective of the nonlinearity and complexity of the system. [24]

## II.5. Transfer learning

Using a trained model's knowledge to learn a new set of data is known as transfer learning (TL). By utilizing information from the source domain and learning task, transfer learning seeks to enhance learning in the target domain. Depending on the kind of task and the kind of data available in the source and target domains, different transfer learning settings are defined.

Transfer learning surpassed state-of-the-art techniques in machine learning. Deep learning has been used in computer-based diagnosis and prediction, mostly due to advances in computer vision. Since transfer learning can function with little to no information during the training phase, it has become increasingly important. In other words, well-established data are modified by moving learning from one from one domain to another. Transfer learning works well in situations where a version performs poorly because there is little or no data. An inductive transfer is the name given to this type of transfer learning in DL. Here, a model match on a distinct but related task is used to practically reduce the reach of feasible models, i.e., model bias. CNNs are used for many different deep learning applications since AlexNet emerged victorious in the ImageNet competition. Researchers have been trying to use CNN for a variety of purposes since 2012. [25]

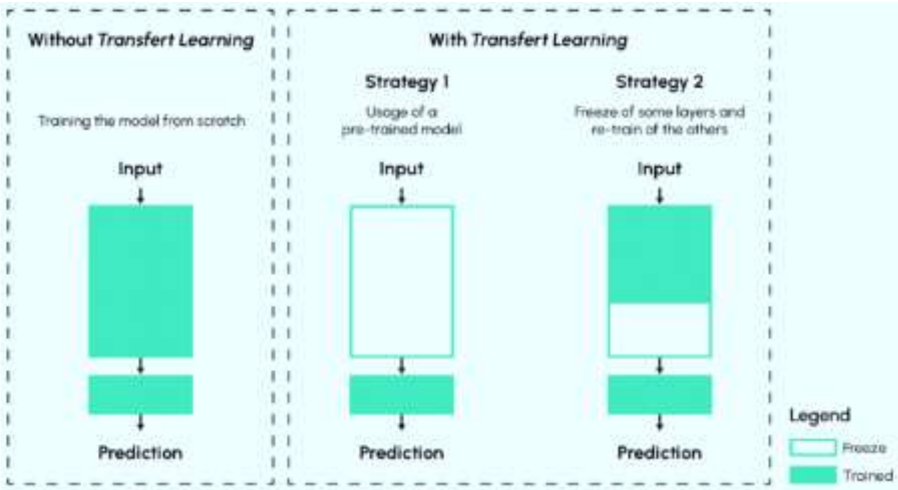


**Figure II.7: Transfer Learning.** [26]

## II.6. Neural Networks for Transfer Learning

### II.6.1. VGG16

Parameter to prevent data overfitting in our trials, we first used the pre-trained VGG-16 convolutional neural network model, which was really modified by freezing parts of the layers. This was especially important for our chosen image set, which is actually quite tiny. The VGG-16 model is a 16-convolutional layer architecture that was put up by Karen in 2014. In terms of the network's input image, it takes the shape of dimensions.

(3 × 224 × 224)Additionally, it has five layers of Max grouping with a size of (2 × 2) across the entire network and sixteen convolutional layers to a fixed size filter in (3 × 3). On the other hand, a softmax output layer is entirely coupled to the top two layers. With over 138 million members, the VGG-16 model regards itself as a sizable network. In order to build deep neural networks that enhance the capacity to learn hidden characteristics, it stacks numerous convolutional layers.

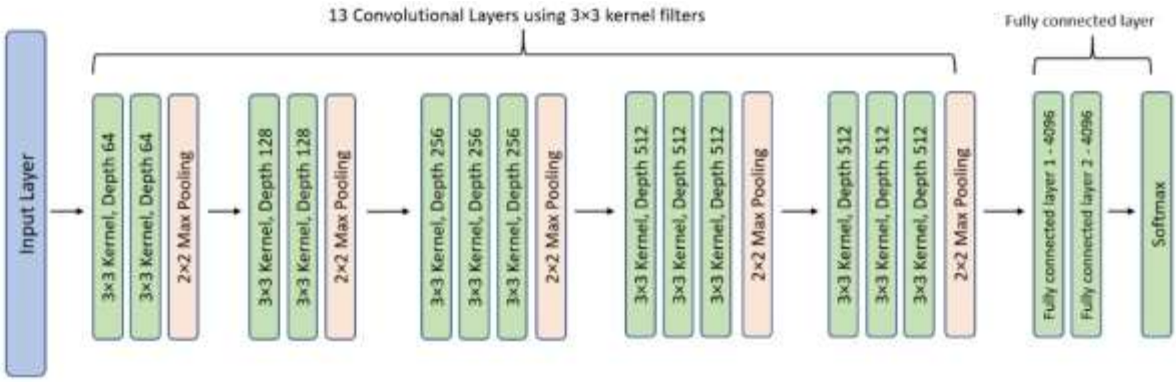


**Figure II.8: VGG-16 model Layers.**

### II.6.2 VGG19

The input of the VGG19 model consists of a 224 × 224 size, 3-channel image with its average RGB value removed. The model has 19 weighted layers, generated by 16 convolutions and 3 fully connected layers (fc). The convolutional layers use a 3 × 3 slot size, with a stride and padding of 1 pixel each. Five max-pooling layers with a 2x2 core size and a 2 pixel stride make up the array.

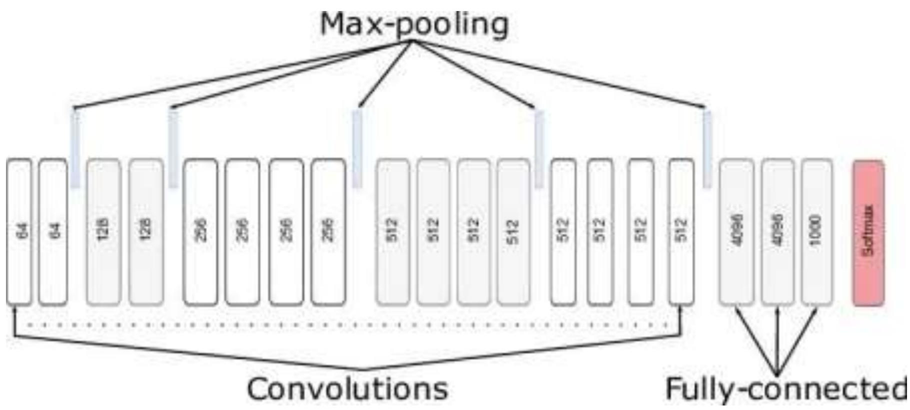


**Figure II.9: VGG-19 model Layers.**

### II.6.3. ResNet50

ResNet50 is a 50-layer residual network. In fact, Microsoft unveiled a deep convolution neural network model in 2015. Instead of learning features in the residual network, we learn residuals, which are the learned features subtracted from the layer inputs. By directly connecting the nth layer's input to the (n+x)th layer, ResNet enables the stacking of further layers and the establishment of a deep network. In our experiment, we employed and improved a pre-trained ResNet50 model. The ResNet50 architecture is shown in Figure (II.10). [27]

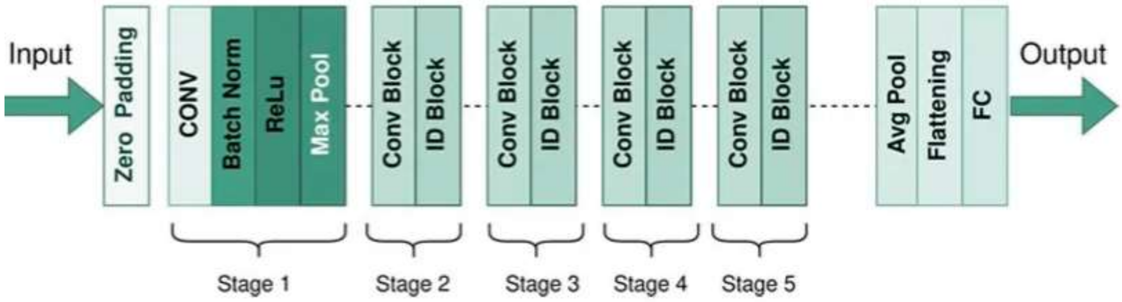


**Figure II.10: ResNet50 model layers. [28]**

### II.6.4. YOLOv8

The firm that created YOLOv5, Ultralytics, launched YOLOv8 in January 2023. YOLOv8 offered five scaled versions: YOLOv8x (extra big), YOLOv8n (nano), YOLOv8s (small), YOLOv8m (medium), and YOLOv8l (large). Numerous vision tasks, including object identification, segmentation, pose estimation, tracking, and classification, are supported by YOLOv8. [29]

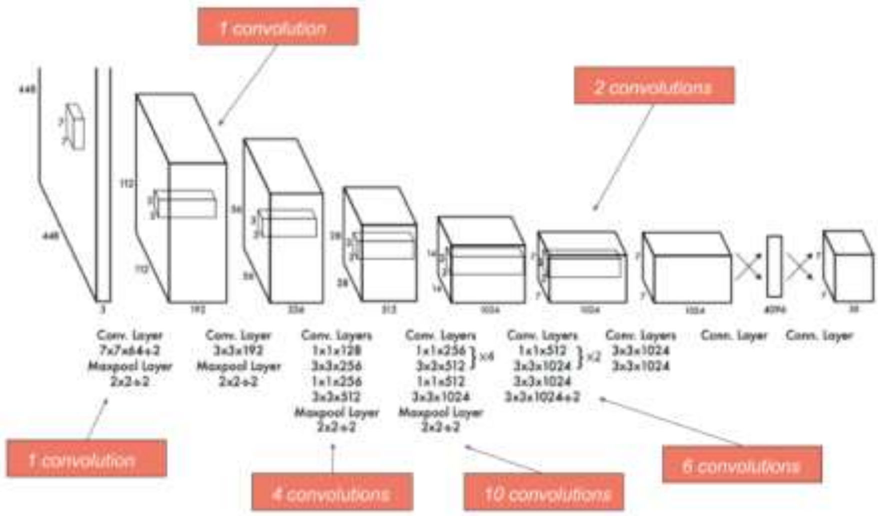


**Figure II.11: The structure of the YOLOv8 model. [30]**

### II.6.5. Discussions

After identifying the previous networks (VGG16, VGG19, ResNet50 and YOLOv8) and training the data on them, the result appears in the form of accuracy and confusion matrix, where we can call this performance indicators.

**Confusion matrix**

Predictive performance is frequently assessed using data analysis in a confusion matrix. This matrix compares how the model identified the various fault categories to how they were really classified (predicted versus observed). This is represented by four sets of data:

- True Positive (TP): An item is predicted to be faulty and it actually is.

- False Positive (FP): An item is expected to be faulty when it is not.

- False Negative (FN): An item is projected as not faulty but is faulty.

- True Negative (TN): An item is predicted as not being faulty, and it is not. [31]

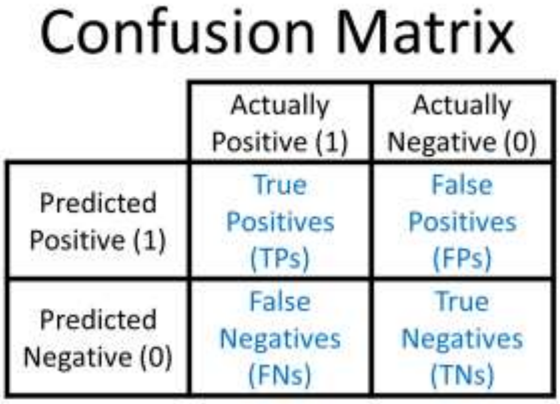


**Figure II.12: Confusion matrix. [32]**

| | | | | | |
|---|---|---|---|---|---|
| Confusion matrix | | True | False | | |
| Class and predictions | True | TP | FP | Precision | = TP/ (TP+FP) |
| | False | FN | TN | Négative Prédictive Value | =TN/ (FN+TN) |
| | | Sensibility = TP/ (TP+FN) | Specificity = TN/ (FP+TN) | Accuracy = (TP+TN)/(TP+FP+TN+FN) | |

**Table II.1: Confusion matrix and formulas.**

**Precision:** The percentage of affirmative cases that were correctly identified.

**Sensibility:** the fraction of true positive cases that are accurately detected.

**Specificity:** the fraction of true negative cases that are correctly identified.

**Accuracy:** the proportion of correct predictions out of the total number.

## II.7. Conclusion

AI is used in many areas, including medicine, to analyze and process images. This is why deep learning and transfer learning should be used to train TB data on networks where this process enables the identification of sick and normal radiation.

# Chapter III

## Experimental results

# III.1. Introduction

AI diagnostic systems can process large amounts of patients' data and deliver results quickly, allowing healthcare providers to make timely decisions and begin appropriate treatment. In this chapter, we will address TB data training on transformative learning networks (VGG16 VGG19 ResNet50 and YOLOv8). Then he went from simulation to implementation where the 'Diatub' app was created to diagnose tuberculosis.

## III.2. Data set description

We have used the publicly accessible Tuberculosis Bacteria (TB) Chest X-ray Database on Kaggle to move forward with the TB detection experimentation. A group of researchers from Qatar University, Doha, Qatar, and Dhaka University, Bangladesh, along with their collaborators from Malaysia and medical professionals from Hamad Medical Corporation and Bangladesh, have developed a database of chest X-ray images for Tuberculosis Bacteria (TB) positive cases as well as normal images. The research team was able to differentiate between normal chest X-ray images and TB images with an accuracy of 98%. Two classes of X-ray pictures totaling 6430 are identified. Normal lungs are represented by the first class, and lungs impacted by tuberculosis bacteria are represented by the second class. But the dataset is unbalanced, with 2930 images showing tuberculosis bacteria infection and 3500 images showing a typical chest X-ray. The image has 512 pixels for height and 512 pixels for width. The dataset's raw photos are displayed in Figure III.1. [33]

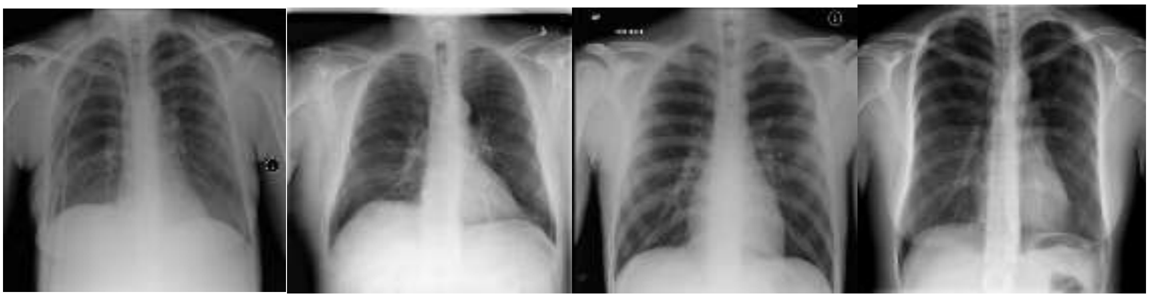

**Figure III.1: Exemplary normal dataset input.**

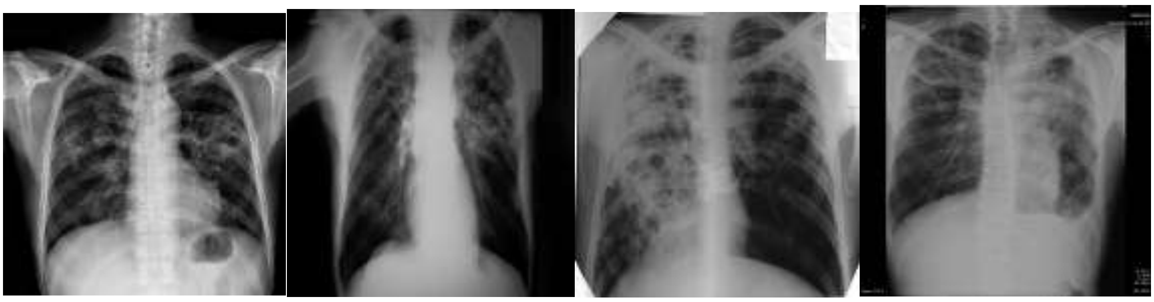

**Figure III.2: Exemplary tuberculosis dataset input. [34]**

### III.2.1. Data preprocessing

Preprocessing is essentially applied to any unprocessed large data set prior to classification or identification. Preprocessing is often necessary since raw data are frequently unusable in real-world scenarios due to noise. The data preparation techniques can result in safe, useable data. [35]

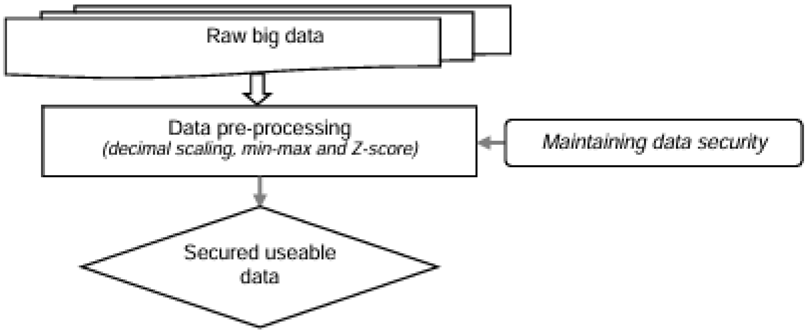


**Figure III.3: A schematic for acquiring a safe and noise-free dataset from large data systems.**

### III.2.2. Data augmentation

To expand the quantity of training data, data augmentation is a popular strategy in deep learning model training. To prevent overfitting and enhance the model's performance, the procedure often entails replacing the images from the current training data. Augmentation techniques are used in the majority of medical research that use chest X-ray datasets in order to enhance model performance.

A review of multiple recent efforts that use particular augmentation techniques to categorize chest X-ray images is shown in Fig. 1. Random rotation and horizontal flip are the most popular augmentations. The most effective methods for categorizing chest X-ray pictures have been determined by comparing augmentation techniques in several investigations. Such as Gaussian blur, rotation, brightness, contrast, random gamma, and horizontal flip. [36]

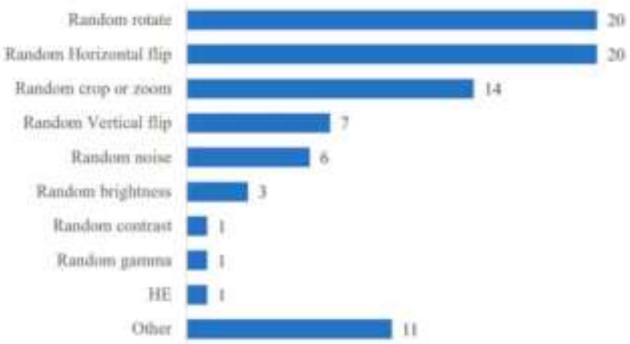


**Figure III.4: These graphs represent various data augmentation techniques.**

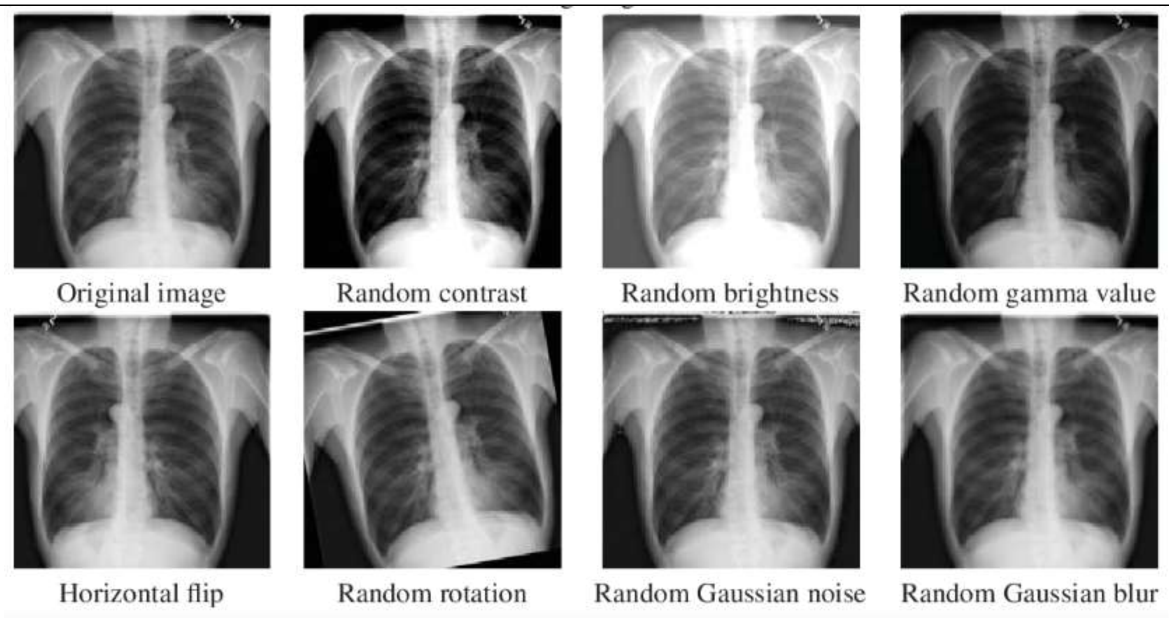


**Figure III.5: Application of data augmentation technique to chest X-ray image. [37]**

## III.2.3. Split of data

Algorithms for machine learning take in patterns from data and apply them to forecast fresh, unknown data. We need to assess our models' performance with data that they haven't seen during training. We'll examine various machine learning data-splitting techniques.

### III.2.3.1. Train Data

The information used to develop our machine learning model is known as train data. The input attributes in this data set are accompanied by corresponding output labels. This data teaches the model patterns, which it then applies to forecast new, unknown data.

### III.2.3.2. Validation Data

This type of data is used to assess how well our model performs during training. To avoid overfitting, we use this data to adjust the hyper parameters of the model. The unseen data that the model will come across in the real world should be reflected in the validation data.

### III.2.3.3. Test Data

Following training and validation, we utilize test data to assess the model's overall performance. To prevent any data leakage, this data should be kept totally apart from the train and validation data. [38]

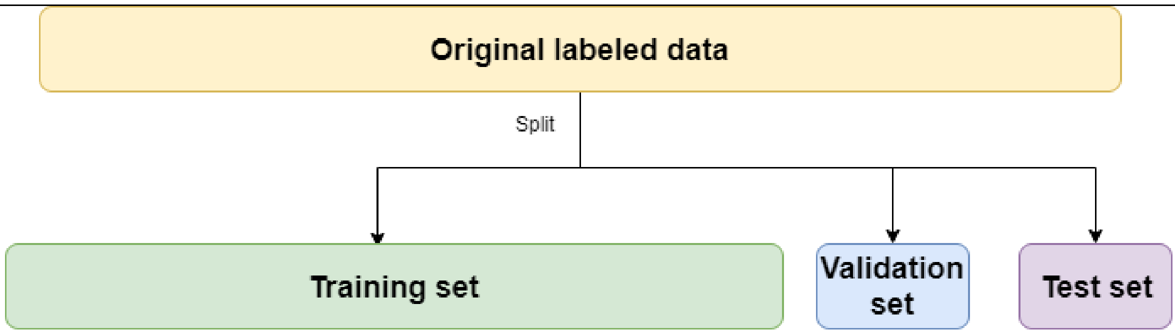


**Figure III.6: Visualization of data-splitting techniques. [39]**

## III.3. Environment of implementation

### III.3.1. Hardware tools

The actual components of a computer, such as the casing, CPU, monitor, mouse, keyboard, and computer data storage, are referred to as computer hardware.

| | |
|---|---|
| Date/heure du jour : | jeudi 30 mai 2024, 10:46:27 |
| Nom de l'ordinateur : | MAROUA |
| Système d'exploitation : | Windows 11 Entreprise 64 bits (10.0, build 22000) |
| Langue : | français (Paramètres régionaux : français) |
| Fabricant du système : | LENOVO |
| Modèle du système : | 20AWS1YT0D |
| BIOS : | GLET95WW (2.49 ) |
| Processeur : | Intel(R) Core(TM) i5-4210M CPU @ 2.60GHz (4 CPUs), ~2.6GHz |
| Mémoire : | 4096MB RAM |
| Fichier de pagination : | 6448 Mo utilisé(s), 1968 Mo disponible(s) |
| Version DirectX : | DirectX 12 |

**Figure III.7: Computer hardware.**

### III.3.2. Software tools

Throughout the entire experiment, Python and Keras were used. With the help of the Keras Library and multi-GPU training capability, models and pre-configured weights may be invoked with a single line order.

The network was created via Google Colab's services.

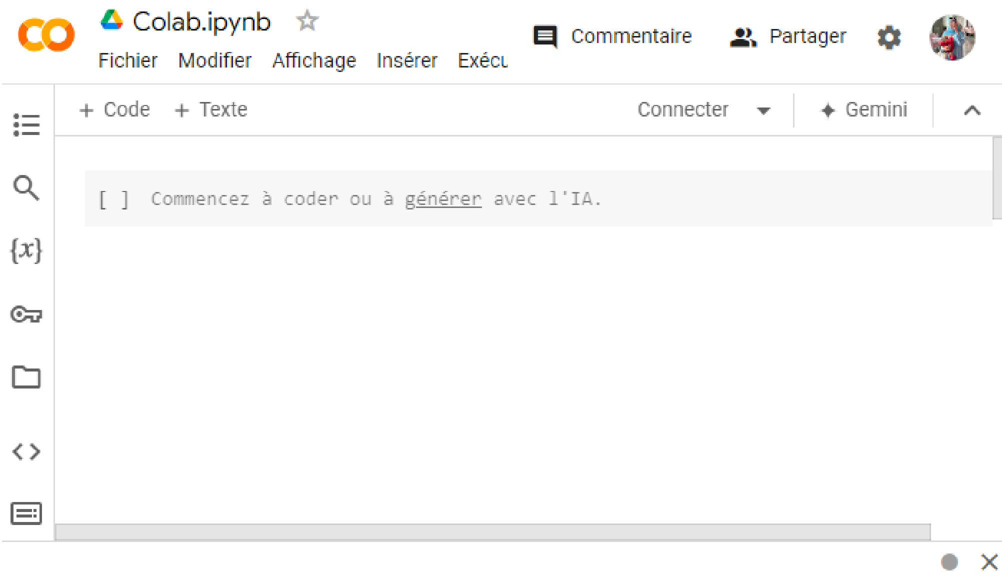


**Figure III.8: Google Colab Interface.**

It has space to write codes, Drive can be connected to Colab so as to raise data

Google Colab was given the following specifications:

- Type of execution is T4 GPU.
- GPU Ram: 15 GB.
- It can be used up to 3 hours continuously.
- System RAM: 12.7 GB.

## III.4. Simulation Results

In this experiment, we trained the tuberculosis database on four networks VGG16, VGG19, ResNet50 and YOLOv8. And now we're going to discuss the results of these network.

### III.4.1. Results of VGG 16

VGG16 were trained in 50 epoch learning transfer, where we added and tuned some layers such as the Pooling layer. The following table shows the structure obtained after the modification of the layers.

| Layer(type) | Output Shape | Param# |
|---|---|---|
| Input_2 (Input Layer) | [(None, 224, 224, 3)] | 0 |
| VGG16 (Functional) | (None, 7, 7, 512) | 14714688 |
| Global_average_pooling2d GlobalAveragePooling2D | (None, 512) | 0 |
| Dense | (None, 2) | 1026 |
| Total params: 14715714 (56.14 MB) | | |
| Trainable params: 1026 (4.01 KB) | | |
| Non-trainable params: 14714688 (56.13 MB) | | |

**Table III.1: The structure obtained after the modification of the layers of VGG16**.

The drive parameters were also selected as follows:

Loss=”binary_crossentropy”, Optimizer=”Adam”, Epochs=50, Metrics=”Accuracy”

After training on the above parameters for 1 hour and 30 min, the following curves were obtained.

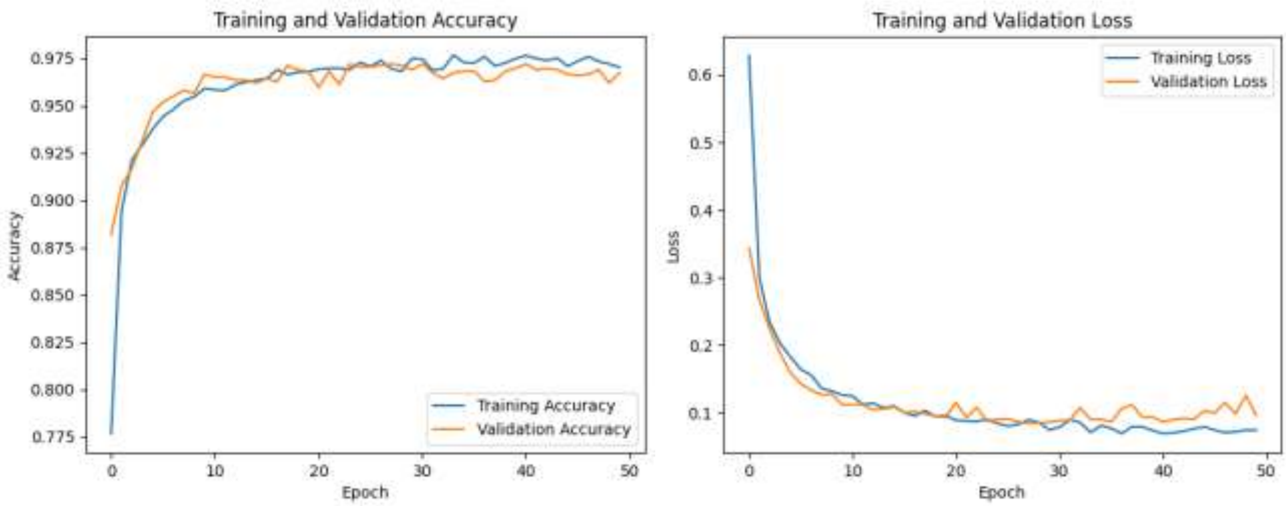


**Figure III.9: Training curves for VGG16.**

The network reached maximum accuracy in training of 97,5% at the beginning of 32 epoch with validation accuracy of about 96%. At the end of the 30 epoch, the network reached the rate of loss of training to 10%, with the rate of loss of validation ranging from 12% to 15%.

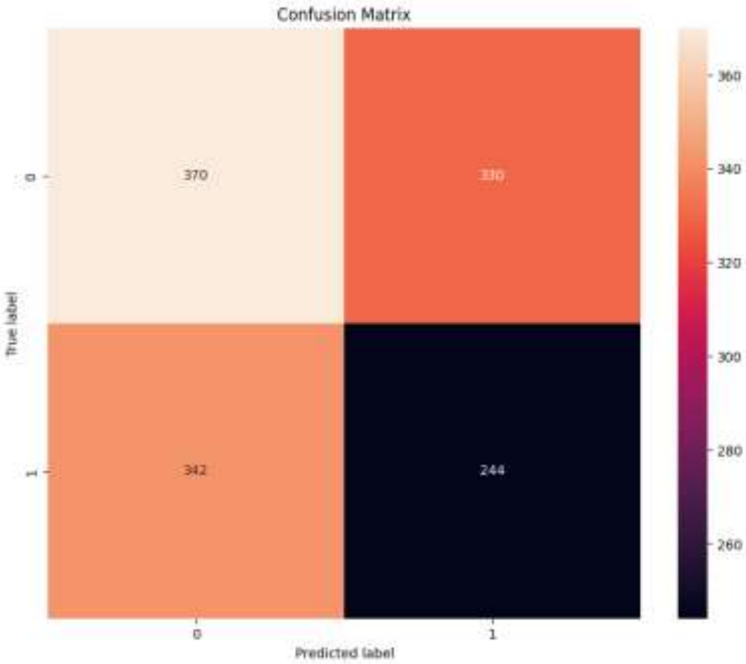


**Figure III.10: VGG16 confusion matrix.**

| | VGG16 confusion matrix | | | |
|---|---|---|---|---|
| **Class and predictions** | **TB** | **No-TB** | **No-Normal** | **Normal** |
| | **370** | **330** | **342** | **244** |
| | **Precision** | **Accuracy** | **Sensibility** | **Specificity** |
| | **0.528** | **789604** | **0.52** | **0.425** |

**Table III.2: illustration VGG16 confusion matrix.**

### III.4.2. Results of VGG 19

VGG19 were trained in 50 epoch learning transfer, where we added and tuned some layers such as the Pooling layer. The following table shows the structure obtained after the modification of the layers.

| Layer(type) | Output Shape | Param# |
|---|---|---|
| Input_4 (Input Layer) | [(None, 224, 224, 3)] | 0 |
| VGG19 (Functional) | (None, 7, 7, 512) | 20024384 |
| Global_average_pooling2d_1 GlobalAveragePooling2D | (None, 512) | 0 |
| Dense_1 | (None, 2) | 1026 |
| Total params: 20025410 (76.39 MB) | | |

| |
|---|
| Trainable params: 1026 (4.01 KB) |
| Non-trainable params: 20024384 (76.39 MB) |

**Table III.3: The structure obtained after the modification of the layers of VGG19**.

The VGG19 network has been trained on the same previous settings and epochs.

The following curves were obtained.

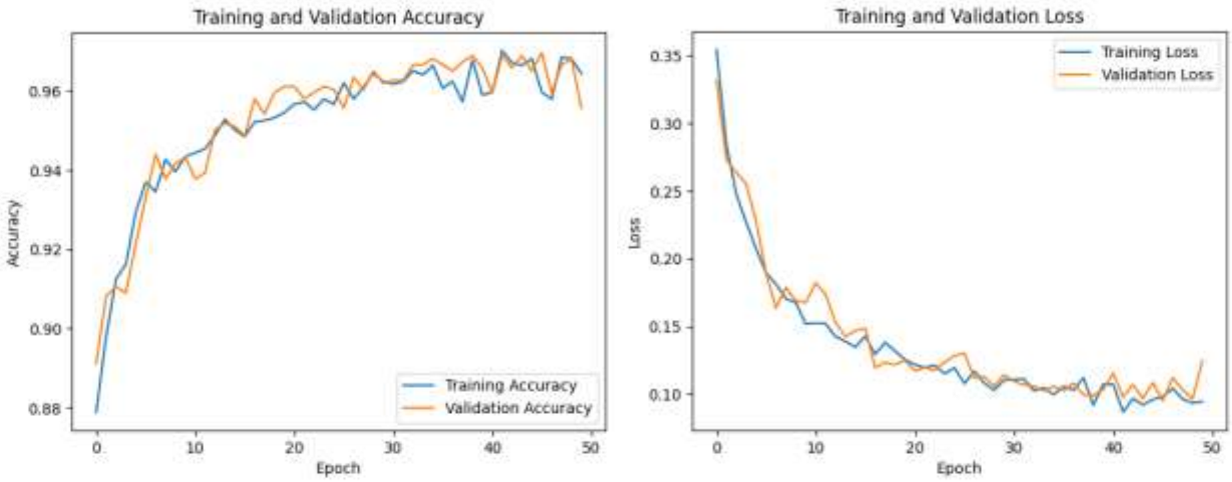


**Figure III.11: Training curves for VGG19.**

The network reached maximum training accuracy of 97% at the beginning of 35 epoch with validation accuracy ranging from 96.1% to 97%. The network reached the rate of loss of training to 10% where the ratio of the epoch ranged from 25 to 50 with the loss of verification at the epoch 10 reached 18% and from the epoch 25 to 50 decreased to 10%.

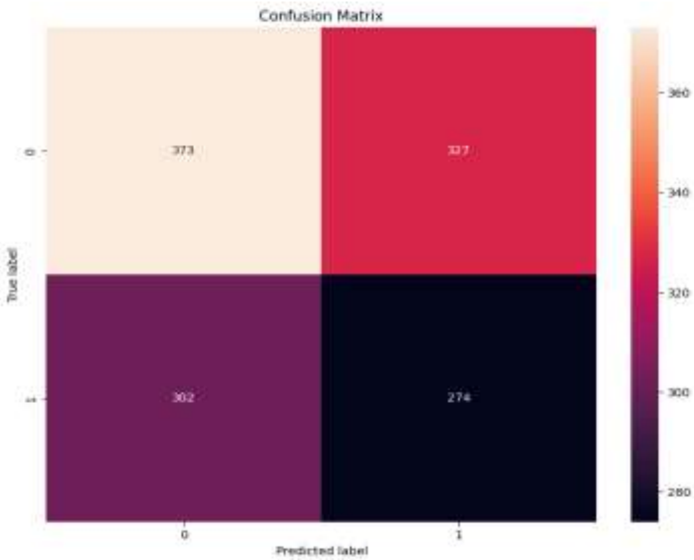

**Figure III.12: VGG19 confusion matrix.**

| VGG19 confusion matrix | | | | |
|---|---|---|---|---|
| **Class and predictions** | **TB** | **No-TB** | **No-Normal** | **Normal** |
| | **373** | **327** | **302** | **274** |
| | **Precision** | **Accuracy** | **Sensibility** | **Specificity** |
| | **0.532** | **827513** | **0.552** | **0.455** |

**Table III.4: illustration VGG19 confusion matrix.**

### III.4.3. Results of ResNet50

ResNet50 were trained in 50 epoch learning transfer, where we added and tuned some layers such as the Pooling layer. The following table shows the structure obtained after the modification of the layers.

| Layer(type) | Output Shape | Param# |
|---|---|---|
| Input_2 (Input Layer) | [(None, 224, 224, 3)] | 0 |
| ResNet50 (Functional) | (None, 7, 7, 2048) | 23587712 |
| Global_average_pooling2d GlobalAveragePooling2D | (None, 2048) | 0 |
| Dense | (None, 2) | 4098 |
| Total params: 23591810 (90 MB) | | |
| Trainable params: 4098 (16.01 KB) | | |
| Non-trainable params: 23587712 (89.98 MB) | | |

**Table III.5: The structure obtained after the modification of the layers of ResNet50.**

The ResNet50 network has been trained on the same previous settings and epochs. The following curves were obtained.

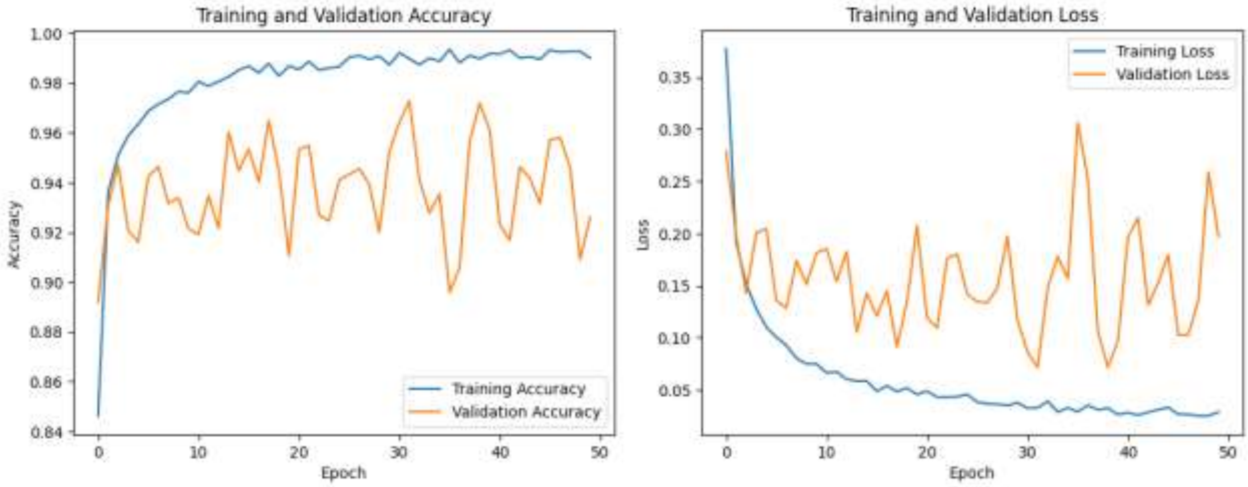


**Figure III.13: Training curves for ResNet50.**

The network reached the maximum accuracy of 99% training from the 10th epoch, while validation rates were variable throughout the epoch reaching 97%. The rate of loss of training was 5%, with the epoch ranging from 18 to 50, with the loss of validation in variable ratios ranging from 8% to 30% throughout the epoch.

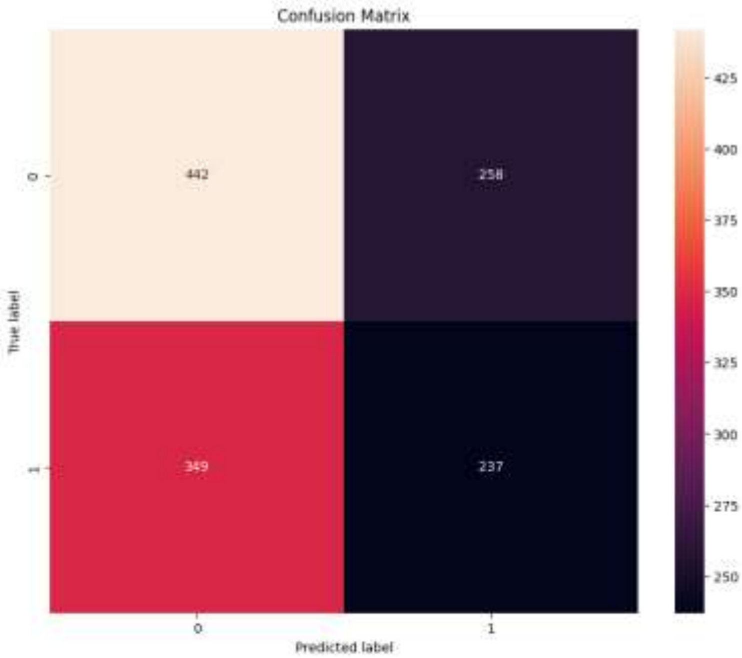


**Figure III.14: ResNet50 confusion matrix.**

| **ResNet50 confusion matrix** | | | | |
|---|---|---|---|---|
| **Class and predictions** | **TB** | **No-TB** | **No-Normal** | **Normal** |

| | | | | |
|---|---|---|---|---|
| | 442 | 258 | 349 | 237 |
| | Precision | Accuracy | Sensibility | Specificity |
| | 0.631 | 873194 | 0.558 | 0.478 |

**Table III.6: illustration ResNet50 confusion matrix.**

### III.4.4. Results of Yolov8

The results obtained from the YOLOv8 training differ from those of previous networks, where YOLOv8 have been trained on criteria somewhat different from those of previous networks because their structure requires it.

50 epoch in each epoch, 16 images are extracted from the batch. The graph obtained through training is shown in the following forms:

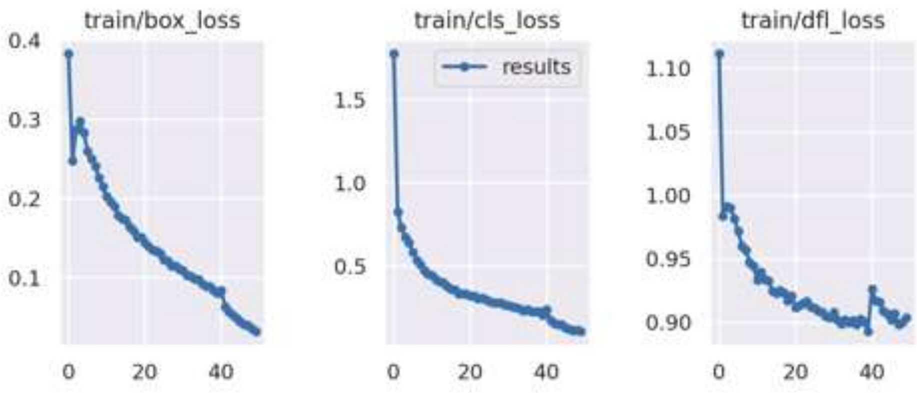


**Figure III.15: YOLOv8 training graphics.**

**Train/box_loss:** Indicates how well the model anticipates an object's bounding boxes. The model's ability to forecast bounding boxes improves as the loss diminishes over the epochs. The **train/cls_loss** ratio indicates how well the model predicts the object class. The loss diminishes as the epochs go by, suggesting that the model is becoming more adept at correctly classifying data. **Train/dfl_loss:** This variable, which aids in the model's learning of object distance, measures the loss related to the distance field loss. The loss diminishes as the epochs go by, suggesting that the model's comprehension of distances is improving.

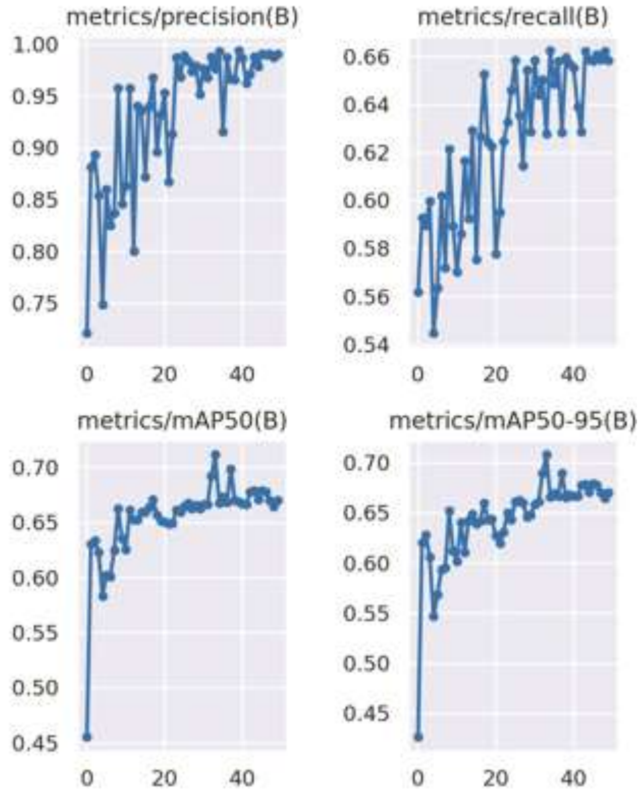


**Figure III.16: YOLOv8 precision/recall graphics.**

**Metrics/precision (B):** This expresses the degree of prediction accuracy provided by the model. When a model has a high precision score, it is generally correctly detecting things.

**Metrics/recall (B):** This quantifies how well the model recognizes every object in a picture. The majority of the items in a picture are detected by the model when it has a high recall score.

**Metrics/mAP50 (B):** This calculates the model's mean Average Precision (mAP) at a 50% confidence level. The performance is improved with a greater mAP.

**Metrics/mAP50-95 (B):** Using a range of confidence criteria from 50% to 95%, this calculates the model's mean Average Precision (mAP). The performance is improved with a greater mAP.

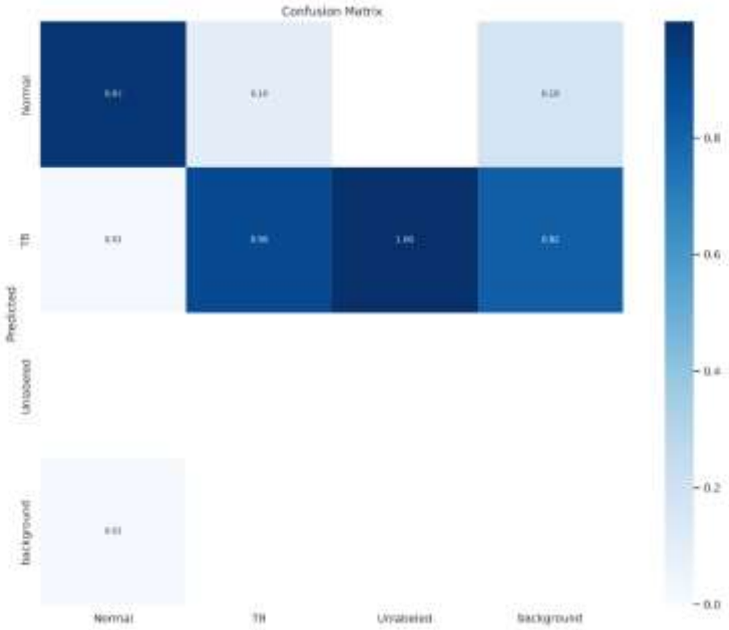


**Figure III.17: YOLOv8 confusion matrix.**

| **YOLOv8 confusion matrix** | | Normal | TB | *Background FP* |
|---|---|---|---|---|
| **Class and predictions** | Normal | 0.97 | 0.10 | 0.18 |
| | TB | 0.01 | 0.90 | 0.82 |
| | Background FN | 0.01 | / | / |

**Table III.7: illustration YOLOv8 confusion matrix.**

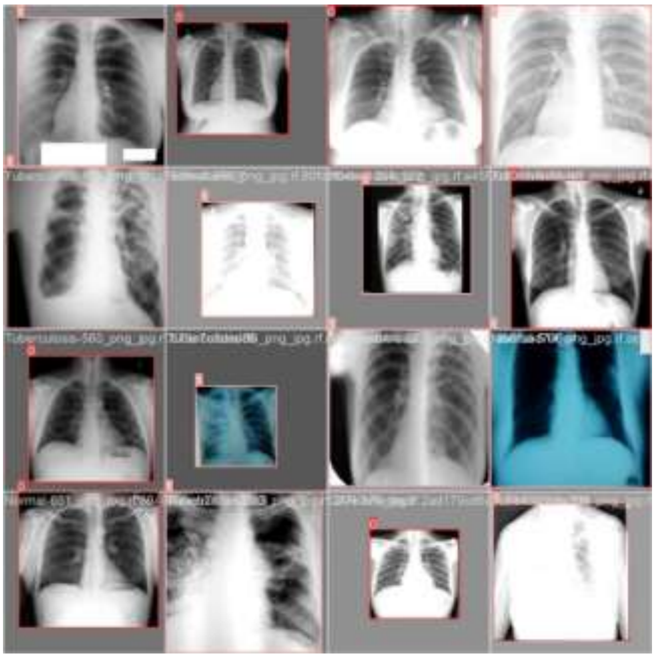

**Figure III.18: Images tested on yolov8 network.**

Some images were tested for ordinary radiation and others were sick with tuberculosis on the yolov8 network, put her square and gave '0' to a normal lung and '1' to a sick lung with tuberculosis.

**Comparison**

Among the previous results, we observed an increase in the accuracy value on the vgg16 and vgg19 networks, as well as a decrease in the accuracy on the yolov8 network.

The accuracy ratio in the network was YOLOv8 large compared to previous networks (VGG16-VGG19-ResNet50) and this network we can determine whether the lung is sick or not.

## III.5. Application of Diagnosis TB 2024

Diatub is an application designed to facilitate early diagnosis of tuberculosis. The application relies on AI-powered image analysis to assess chest X-ray, making it possible for healthcare workers of various levels of expertise to reach a more accurate diagnosis.


**Figure III.19: Application logo.**

### III.5.1. Description of the application

The Diatub app has several stages to reach the final result starting from login. This by inserting the username and password after which we go to the next page which is the data entry form then we find workspace divided into two sections to raise the X-ray image of the lung and the other section of the output and also provided with icons to download and lift the radiation and the other to process and then the result appears can be saved with a save icon, as well as an icon to exit.

The outputs of this application are the previous Chinese radiation and the item in the sense that this radiation is sick with tuberculosis or a normal lung, also accompanied by a percentage, which means the extent to which the application recognizes the lung condition, whether sick or ordinary.

### III.5.2. Interfaces of the application

Offer in Figure (III.20) Next Steps to Work in the ‘Diatub’ App

(A)

(B)

(C)

(D)

(E)

(F)

(G)

**Figure III.20: Stages of diagnosis of TB in Diatub.**

**(A):** Login Interface.

**(B):** Login confirmation interface.

**(C):** Data entry form.

**(D):** Workspace for data lifting.

**(E):** Upload X-ray image of lung.

**(F):** Image appearance on the worktop.

**(G):** The app processes the image and shows the result.

### III.5.3. Testing the application

In order to test Diatub app take first the image to be tested.

**Figure III.21: X-ray image to be tested.**

Then we upload it to Diatub and process it.

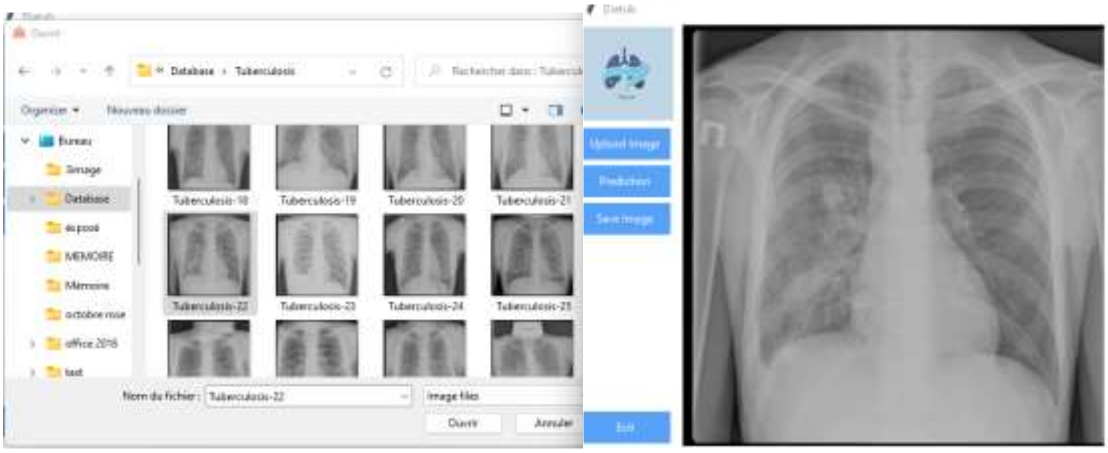

**Figure III.22: Upload Data.**

After the X-ray is lifted, Diatub processes it using artificial intelligence and gives the following result:


**Figure III.23: Diatub result.**

## III.6. Conclusion

At the end of this project we have been able to create an app that helps in the early detection of tuberculosis disease under the name 'Diatub' using AI and image processing techniques. This app is the first version as we can modify and improve it in the future by adding some services such as:

- There is an awareness-raising aspect about tuberculosis as well as the necessary precautions to avoid it or a message of optimism.
- Add other TB types so it doesn't just depend on lung TB.
- Add some infectious chest diseases.

# General Conclusion

Due to the high prevalence and seriousness of tuberculosis in the world, the difficulty of detecting it and the expensive cost of analyses because of the inability of a group of patients to afford these costs, we have proposed a way to help patients take a relative result of his condition in a short time and also to save mobility time and also contribute to relieving pressure on doctors and specialists to detect the disease.

Technological development has revolutionized the scientific field. Through the development of advanced computing and data transfer, this is due to artificial intelligence and its use in several areas, including the field of medicine, which has helped in the addition of new technologies, including the detection of some diseases using artificial intelligence and its branches, which are machine learning, deep learning and also include the transfer learning.

We have seen that many works involved artificial intelligence to solve practice problems, including health problems and disease detection. There for we have try to use several training model as (VGG16-VGG19-ResNet50-YOLOv8), his gives us a good results then we transfer from simulation to implementation.

The Diatub app works by imaging the lung X-ray and then lifting it in the app. After treatment, the result is the patient's state of health, whether in a sick or normal condition, linked to the ratio of application knowledge of the disease and all this in a short time and with high accuracy.

This software is the initial version, and we plan to add more features and updates in the future, like:

- Raising awareness about tuberculosis and the steps to prevent it, as well as a positive message.
- Don't rely solely on pulmonary TB.
- Include other forms of tuberculosis.
- Include a few contagious thoracic illnesses.

# List of references


[1] Daniel, T. M., Bates, J. H., & Downes, K. A. (1994). History of tuberculosis. Tuberculosis: pathogenesis, protection, and control, 13-24.

[2] Pai, M., Behr, M. A., Dowdy, D., Dheda, K., Divangahi, M., Boehme, C. C., Ginsberg, A., Swaminathan, S., Spigelman, M., Getahun, H., Menzies, D., & Raviglione, M. (2016). Tuberculosis. Nature Reviews. Disease Primers, 2, 16076.doi.org/10.1038/nrdp.2016.76.

[3] https://radioalgerie.dz/news/fr/article/20210324/209058.html.

[4] https://radiopaedia.org/articles/tuberculosis-pulmonary-manifestations-1.

[5] Campo, M., & Kawamura, L. M. (2017). What is tuberculosis (TB)? American journal of respiratory and critical care medicine, 195(4), P7-P8

[6] https://fr.vecteezy.com/art-vectoriel/1988683-tuberculose-symptomes-information-infographie.

[7] Nardell, Edward A.ell. Tuberculosis (TB). Invited review series: tuberculosis, 2022, www.msdmanuals.com/home/infections/tuberculosis-and-related-infections/tuberculosis-tb.

[8] TST, T. S. T. Testing for tuberculosis (TB).

[9] https://www.healthcarefinancenews.com/news/experts-blood-test-more-efficient-cheaper-way- spot-tuberculosis

[10] Konstantinos, A. (2010). Testing for tuberculosis. Australian prescriber, 33(1).

[11] https://www.myamericannurse.com/tb-tuberculin-skin-test-interpretations/

[12] https://www.mutupelayanankesehatan.net/13-berita/3071-how-do-you-read-a-tb-skin-test

[13] World Health Organization. (2016). Chest radiography in tuberculosis detection: summary of current WHO recommendations and guidance on programmatic approaches. World Health Organization. https://iris.who.int/handle/10665/252424.

[14] Francis, M. (2020). Overview of image processing (p. 6). : Overview of image processing overview of image processing contents. 10.13140/rg.2.2.23374.89929.

[15] Khenfer, i., Bettayeb, e. a., & Salhi, D. E. H. Filtrage Adaptatif 2-D pour la Restauration d'images perturbées par du Bruit Impulsionnel (Doctoral Dissertation, Université Kasdi Merbah Ouargla).

[16] Valavanidis, A. Artificial Intelligence (AI) Applications

[17] Manning, Christopher. Stanford University Human-Centered Artificial Intelligence. Artificial Intelligence Definitions, 2020.

[18] BEKKARI, L., & KADI, N. Détection D'incendie Et De Fumée A L'aide De L'apprentissage Par Transfert (Fire and Smoke Detection Using Transfer Learning (Doctoral dissertation, UNIVERSITY OF KASDI MERBAH OUARGLA).

[19] Old, O., Friedrichson, B., Zacharowski, K., & Kloka, J. A. (2023). Entering the new digital era of intensive care medicine: an overview of interdisciplinary approaches to use artificial intelligence for patients' benefit. European Journal of Anaesthesiology and Intensive Care, 2(1), e0014.

[20] Gadde, S. S., & Kalli, V. D. (2021). Artificial Intelligence and its Models. International Journal for Research in Applied Science & Engineering Technology, 9(11), 315-318.

[21] Yamashita, R., Nishio, M., Do, R. K. G., & Togashi, K. (2018). Convolutional neural networks: an overview and application in radiology. *Insights into imaging*, *9*, 611-629.

[22] Ghosh, A., Sufian, A., Sultana, F., Chakrabarti, A., & De, D. (2020). Fundamental concepts of convolutional neural network. Recent trends and advances in artificial intelligence and Internet of Things, 519-567.

[23] Gholamalinezhad, H., & Khosravi, H. (2020). Pooling methods in deep neural networks, a review. ArXiv preprint arXiv: 2009.07485.

[24] Alzubaidi, L., Zhang, J., Humaidi, A. J., Al-Dujaili, A., Duan, Y., Al-Shamma, O. ... & Farhan, L. (2021). Review of deep learning: concepts, CNN architectures, challenges, applications, future directions. Journal of big Data, 8, 1-74

[25] Lôbo Marques, João Alexandre, et al. *Cognitive and Soft Computing Techniques for the Analysis of Healthcare Data*. Artificial neural network-based approaches for computer-aided disease diagnosis and treatment, 2022, pp. 79-99, doi.org/10.1016/B978-0-323-85751-2.00008-6.

[26] https://www.linkedin.com/pulse/transfer-learning-convolutional-neural-networks-alwan/.

[27] Kamal, K., & Hamid, E. Z. (2023). A comparison between the VGG16, VGG19 and ResNet50 architecture frameworks for classification of normal and CLAHE processed medical images.

[28] https://medium.com/@arashserej/resnet-50-83b3ff33be7d.

[29] Terven, J., Córdova-Esparza, D. M., & Romero-González, J. A. (2023). A comprehensive review of yolo architectures in computer vision: From yolov1 to yolov8 and yolo-nas. Machine Learning and Knowledge Extraction, 5(4), 1680-1716.

[30] https://blent.ai/blog/a/detection-images-yolo-tensorflow.

[31] Bowes, D., Hall, T., & Gray, D. (2012, September). Comparing the performance of fault prediction models which report multiple performance measures: recomputing the confusion matrix. In Proceedings of the 8th international conference on predictive models in software engineering (pp. 109-118).

[32] Measuring Performance: The Confusion Matrix – Glass Box (glassboxmedicine.com).

[33] Rima, S. A., Zannat, M., Haque, S. S., Kawsar, A., Jennifer, S. S., & Reza, A. W. (2023, August). Tuberculosis Bacteria Detection Using Deep Learning Techniques. In International Conference on Image Processing and Capsule Networks (pp. 297-308). Singapore: Springer Nature Singapore.

[34] https://www.kaggle.com/datasets/scipygaurav/tuberculosis-tb-chest-x-ray-cleaned-database?select=TB+Chest+Radiography+Database.

[35] Rahman, A. (2019). Statistics-based data preprocessing methods and machine learning algorithms for big data analysis. International Journal of Artificial Intelligence, 17(2), 44-65.

[36] Chokchaithanakul, W., Punyabukkana, P., & Chuangsuwanich, E. (2022). Adaptive image preprocessing and augmentation for tuberculosis screening on out-of-domain chest X-Ray dataset. IEEE Access, 10, 132144-132152.

[37] Sirazitdinov, I., Kholiavchenko, M., Kuleev, R., & Ibragimov, B. (2019). Data Augmentation for Chest Pathologies Classification. *2019 IEEE 16th International Symposium on Biomedical Imaging (ISBI 2019)*, 1216-1219.

[38] https://www.linkedin.com/pulse/data-splitting-strategies-machine-learning-swapnil-sharma/.

[39] https://www.brainstobytes.com/test-training-and-validation-sets/.